IJMF, Iranian Journal of Materials Forming, Vol.1, No.1, pp. 46-55
Printed in The Islamic Republic of Iran, 2014

Failure Prediction during Uniaxial Superplastic Tension Using Finite Element Method

M. E. Hosseini, S. J. Hosseinipour * and M. B. Jooybari
Department of Mechanical Engineering, Babol Noshirvani University of Technology, Babol, Iran.

Abstract: Superplastic materials show a very high ductility. This is due to both peculiar process conditions and material intrinsic characteristics. However, a number of superplastic materials are subjected to cavitation during superplastic deformation. Evidently, extensive cavitation imposes significant limitations on their commercial application. The deformation and failure of superplastic sheet metals are a result of a combination and interaction process between tensile instability and internal cavity evolution. Thus, this study carried out modeling of the uniaxial superplastic tensile test using a code based on the finite element method, that used a microstructure based constitutive model and a deformation instability criterion. These models are the criterion account for both geometrical instabilities and cavitation. It is observed that the proposed approach captures the characteristics of deformation and failure during superplastic forming. In addition, the effects of the cavitation on the superplastic forming process were investigated. The results clearly indicated the importance of accounting for these features to prevent premature failure.

Keywords: Superplastic forming, failure, cavitation, instability, finite element method

1. Introduction

There is a continuing tendency toward the weight reduction of vehicles in these years. Aluminum alloys have primary potential for lightweight structural application in the shipbuilding, automotive, and aerospace industries. For these applications, non-heat treatable AA5083 is preferred because of its reasonable strength, good corrosion resistance, weldability, and ability to take surface finishes. The alloy's formability at room temperature is very low and it is impossible to make a complicated shape. In order to overcome such problems, the hot forming of the aluminum alloy sheets with different forming processes was promoted, and it has been investigated for several decades.

Superplasticity is defined as the ability of polycrystalline materials to exhibit high elongation prior to failure. Generally, superplastic materials are used in vehicle and aerospace industries, which are interested in the parts with characteristics of both structural efficiency and light weight. Other industries are showing interest in producing complex shapes with few mechanical steps [1,2]. The high ductility of superplastic materials is due to both process conditions and material characteristics. The forming temperature should be greater than about half the material absolute melting point and the strain rate should be low, generally between 10^{-5} and 10^{-3} s^{-1}. Moreover, the material should have a fine and stable grain size. It is observed that the value of the strain rate sensitivity index (m) has a strong effect on the ductility of superplastic materials. In general, the higher the m value, the greater the elongation to failure [3–5]. Shehata et al. [6] examined the formability of several Al-Mg alloys from room temperatures to 300°C over a wide range of strain rates by performing uniaxial and biaxial stretch forming tests. Naka et al. [7] investigated the effect of forming speed and temperature on the formability of AA5083 alloy sheet by stretch forming tests with a flat head cylindrical punch at various forming speeds and temperatures

Received by the editors December 30, 2013;Revised February 4, 2014 and Accepted February 23, 2014
* Corresponding author (Email: j.hosseini@nit.ac.ir)

from room temperature to 300 °C. Hosseinipour [8] studied the hot deformation behavior of AA5083 with tensile tests at various temperatures and strain rates. The results showed that the formability increased with decreasing speed for any strain paths at high temperatures, while at room temperature it was not that much sensitive to speed. Hosseinipour [9] investigated the strain rate sensitivity and cavitation in a commercial 5083 aluminum alloy. The results showed that with increasing temperature, the maximum strain rate sensitivity decreases and shifts to the lower strain rates. The failure surface is wide and failure occurs by cavitation. Chung and Cheng [10] showed that, in some superplastic materials, the fracture mode is dominated by unstable plastic flow. The instability of superplastic deformation was studied by several investigators through analytical approaches. Pearce [11] showed that in the tensile test the shrinkage rate is inversely proportional to the cross section of the specimen and highly sensitive to the strain rate sensitivity index.

A significant problem during superplastic forming process is the failure mode of sheet metals. During superplastic flow, a material fails by two possible mechanisms; plastic flow instability, and cavitation. In the present study, using a code based on the finite element method, the modeling of superplastic failure was carried out; using a microstructure based constitutive model and both plastic flow instability and cavitation criterion. The uniaxial superplastic tensile test of AA5083 alloy sheet were simulated numerically.

2. Finite element simulation

The analysis of plastic flow instability is performed by using Marciniak and Kuczynski [12] model. They purposed that the thinning in the tensile specimen can be assumed to be the result of the pre-existing geometrical or structural non-homogeneity which can grow under the imposed deformation. This non-homogeneity may be associated to a variation of the sheet thickness or some defects of the lattice. The rate of thinning in the tensile specimen is therefore determined by the size of the non-homogeneity, and also the strain rate sensitivity index value. Therefore, according to Fig. 1, the specimen has two regions: region ‘‘A’’ having an initial uniform thickness t_0^A and region ‘‘B’’ having an initial thickness t_0^B.

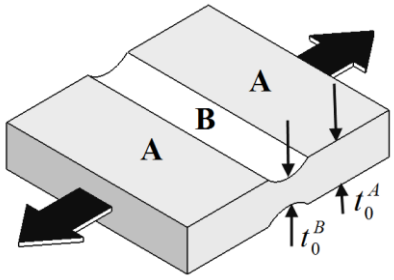

Fig.1. Geometrical model of sheet metal.

The model is based on the growth of the geometrical non-homogeneity. The initial value of the geometrical defect is characterized by the ratio of $f_0 = t_0^B / t_0^A$. This material is subjected to superplastic deformation applying a constant velocity at the region ‘‘A’’ of the specimen. During superplastic flow, the evolution of strain rates is different in the two zones. If ε_1^A and ε_1^B are the principal strains in the two

regions, when the ratio $\varepsilon_1^B/\varepsilon_1^A$ becomes too high, the limiting strain of the sheet is reached. The principal strain ε_1^A in region ‘‘A’’ represents the limit strain.

The analysis of cavity damage model is performed using Stowell [13] model, assuming a certain level of pre-existing voids within the material. The micro voids are pre-existing inside the superplastic materials, which are produced from thermo-mechanical treatments to get fine-grained structures. The presence of micro structural defects contributes to void nucleation. A cavity during superplastic flow may grow by plastic deformation of the surrounding matrix (plasticity-controlled growth). Therefore, the cavity grow was given by

$$C_v = C_0 \exp(\eta\varepsilon) \tag{1}$$

Where C_0 is the initial volume fraction of cavities and η is the cavity growth rate. Finite element software ABAQUS v6.9 was used to predict the fracture of uniaxial superplastic tensile test and biaxial superplastic bulge test of AA5083 alloy at 450, 500 and 550 ^oC using the CREEP mode. The geometrical model of FEM uniaxial superplastic tensile test is illustrated in Fig. 2

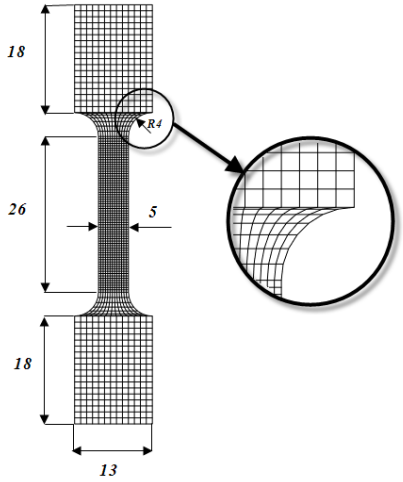

Fig.2. Geometrical models of FEM uniaxial superplastic tensile test (Dimensions in mm).

The element type CPS4R was used in the FEM simulations. This is a 4-node bilinear plane stress quadrilateral, reduced integration, and hourglass control element. 1520 elements with 1652 nodes were defined. The element shape is quad and the technique of meshing is structured. The simple tensile test sample displayed in Fig.2, which is clamped at the bottom and the top side is stretched with a velocity according to the defined strain rate. This velocity can be calculated as follow;

$$v = \dot{\varepsilon}.L \tag{2}$$

Where L is the instantaneous length of the sample and $\dot{\varepsilon}$ is the constant strain rate. Thus, a power law form of the constitutive relationship is assumed:

$$\bar{\sigma} = C\dot{\bar{\varepsilon}}^m \tag{3}$$

Where $\bar{\sigma}$ is the effective stress, $\dot{\bar{\varepsilon}}$ is the effective strain rate, C is a constant, and m is the strain rate sensitivity index.

The material characteristics in the hot condition were determined by bulge tests with the gas blow forming process at various temperatures and pressures using the following equation [14, 15]:

$$m = \frac{ln(P_1 / P_2)}{ln(t_2 / t_1)} \tag{4}$$

where t_1 and t_2 are the forming times necessary to obtain the same dome height at constant pressures of P_1 and P_2, respectively. The dome height during the bulge test was measured by an ultrasonic telemetry sensor.The equivalent stress, strain and strain rate in the dome apex were calculated using the following equations [16, 17]:

$$\bar{\sigma} = \frac{pr}{2s} \tag{5}$$

Where

$$r = \frac{h^2 + (d/2)^2}{2h} \tag{6}$$

And

$$\bar{\varepsilon} = ln\frac{s}{s_0} \tag{7}$$

And

$$\dot{\bar{\varepsilon}} = \frac{\bar{\varepsilon}}{t} \tag{8}$$

where r is the dome radius, s is the final thickness of the dome apex, s_0 is the initial thickness of the blank, h is the dome height, d is the die diameter, and t is the forming time.

Using these two criteria, plastic flow instability and cavity damage model, the fracture of commercial *Al5083* at 450, 500 and 550 ^{o}C under simple tensile test have been predicted through finite element method. In the finite element software, *ABAQUS v6.9*, the constitutive law of material, cavitation and instability of material have been implemented using the *CREEP* and *SDIVINI* subroutines. The constants of Eq. 1 and Eq. 3 obtained from experimental tests are shown in tables 1 and 2 respectively.

Table 1. The values of Eq 1. constants obtained by experimental test

Critical cavity volume fraction(C_V)	Initial volume fraction (C_o)	Void growth parameter (η)
0.30	0.018	2.05

Table2. The constants of Eq (3) at various temperatures

Temp ^{o}C	m	C(MPa)
450	0.32	138.9
500	0.35	116.9
550	0.34	68

Eq. 1. has been implemented in SDIVINI subroutine to define the cavitation phenomenon as a fracture factor. SDVINI, is a user subroutine in ABAQUS v.6.9 to define initial solution-dependent state variable fields. User subroutine SDVINI was called for user-subroutine-defined initial solution-dependent state variable fields at particular material points, shell section points, contact slave nodes, or for user elements. This subroutine can be used to initialize solution-dependent state variables allocated .It returns a value of zero for any solution-dependent state variables that have no defined initial condition. Solution-dependent state variables initialized in SDVINI can be used and updated in the following user subroutines: CREEP, FRIC, HETVAL, UEL, UEXPAN, UGENS, UHARD, UMAT, UMATHT, USDFLD, UTRS. These variables are passed into these routines in the order in which they are entered in SDVINI [18].

The fracture criterion (Eq.1) and the unstable plastic flow $(\varepsilon_1^B / \varepsilon_1^A = 10)$ have been implemented in FEM using Fortran 9.1 compiler. This code has been interfaced with ABAQUS with the graphical interface software, VISUAL STUDIO V.2005. The discaused link and the calculating procedure is illustrated in Fig.3.

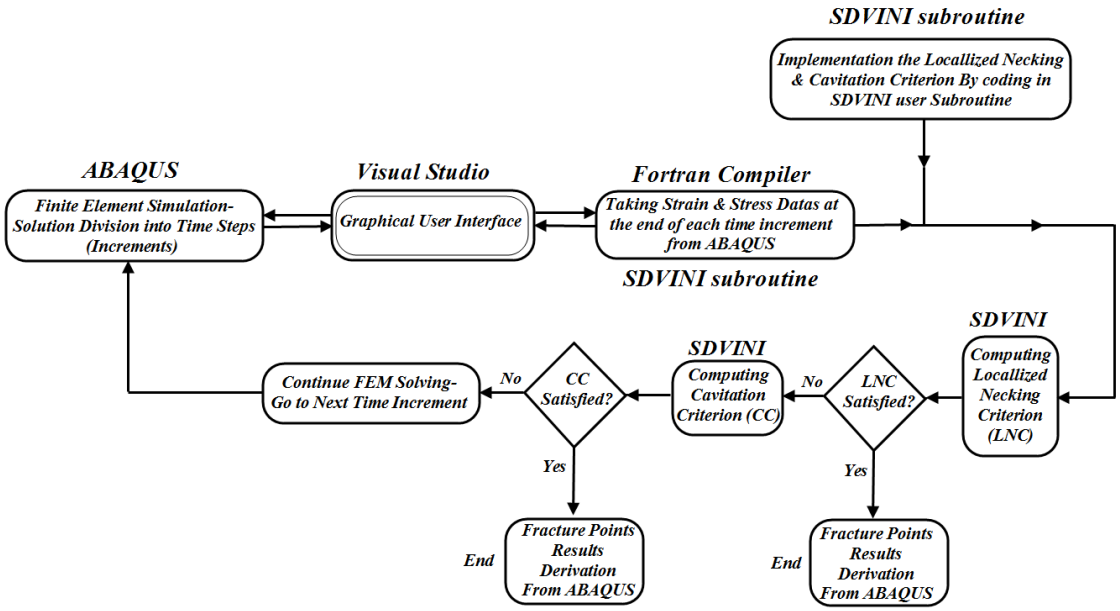

Fig.3. ABAQUS, Visual Studio & Fortran Compiler link to implement failure criterions.

3. Results and Discussions

Fig. 4 and 5 indicate the material constants at elevated temperatures and various strain rates, which were obtained by bulge tests using the gas blow forming process. The material constants were calculated at different dome heights, and the mean values were reported. As can be seen, with increasing temperature the *m* value increased, and the maximum *m* value was obtained at 500 °C, but the *C* constant decreased as the temperature increases.

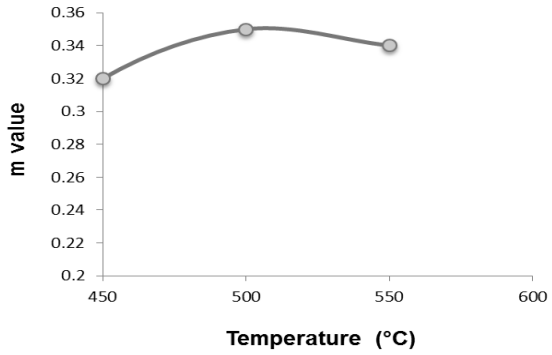

Fig. 4. The *m* value at various temperatures.

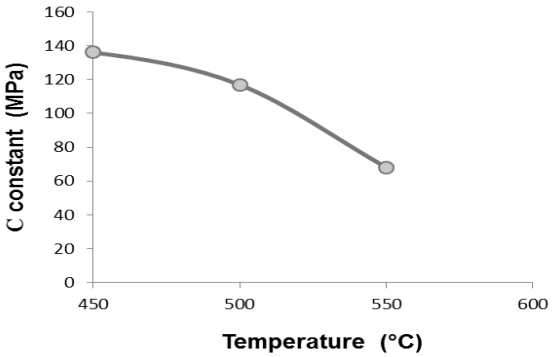

Fig. 5. The *C* constant at various temperatures.

In order to verify the results of FEM, the elongation of hot tensile tests at $450^{o}C$ and strain rates of $10^{-3}, 1.2\times10^{-3}, 1.4\times10^{-3}, 1.7\times10^{-3}$ and $10^{-2}\,s^{-1}$ have been compared with the experimental results of Ref.[8]. As it is shown in Fig.6, the comparison indicates a good accordance between FEM and experimental findings.

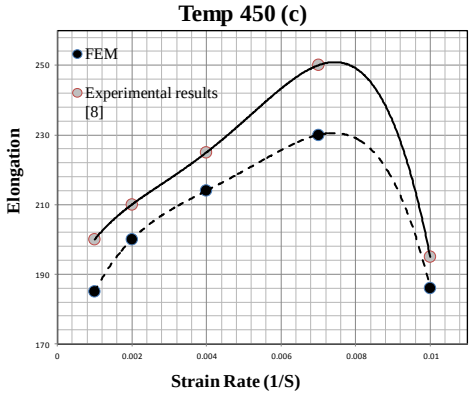

Fig.6 The variation of elongations versus strain rate.

In numerical analysis, the *f* values from 0.999 to 0.99 as well as 1 are considered. The effects of material constants (*C*, *m*) and the specimen geometry were analyzed. The *m* value has been varied from 0.32 to 0.35. The numerical results have shown that the strain localization phenomenon is independent

from the *C* value and it depends on the geometry of the specimen. Fig. 7 shows the predicted limit strains at different *m* values.

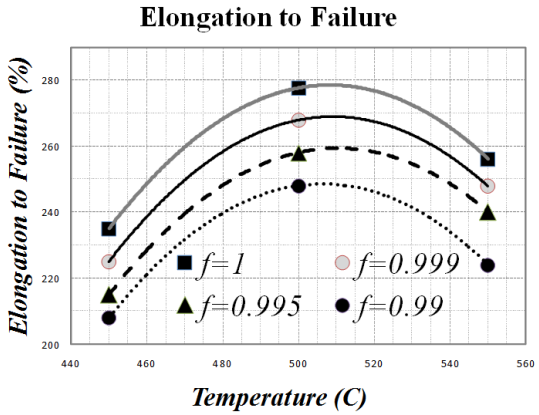

Fig. 7. Elongation to fracture (%) for different f values.

It is shown that in both initial non-homogeneity factors, the predicted strain increases with increasing *m* value. If a small value of initial non-homogeneity factor is assumed, the predicted limit strain decreases. Fig. 8 illustrates the specimen after hot tension test with about 250% elongation.

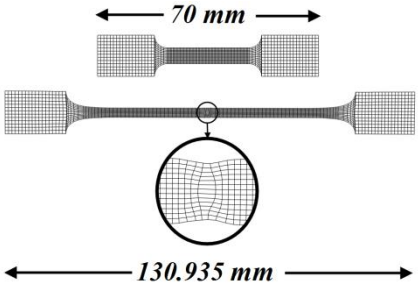

(a)

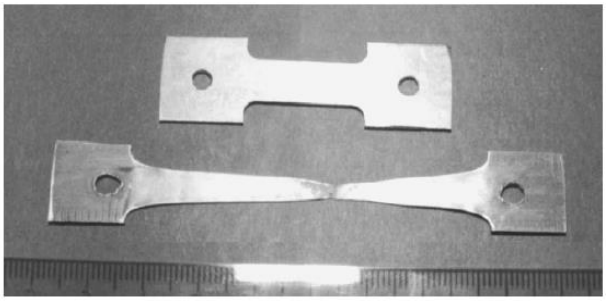

(b)

Fig.8 Comparing the tensile specimens before and after tensile test at 450 ^{o}C . a) FEM b) experimental result [8].

In Fig. 9 the deformed samples at 450, 500 and 550 ^{o}C and their contours of equivalent creep strain have been shown. It is observed that at 450 ^{o}C (*m*=0.32) the localized necking is the effective factor on the fracture, but at 500 and 550 ^{o}C (by increasing the temperature), the cavitation is the main factor for

the fracture. Simple tensile test of Al-5083 has been implemented at 450 ^{o}C at three strain rates: 10^{-1}, 10^{-3} and 10^{-5} s^{-1}.

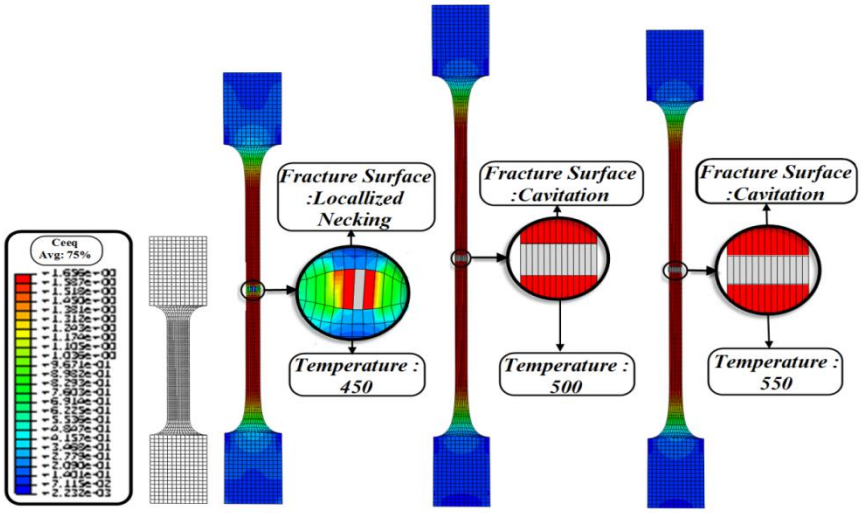

Fig. 9. Deformed simple tensile test specimens at 450, 500 and 550 ^{o}C and 10^{-2} s^{-1}.

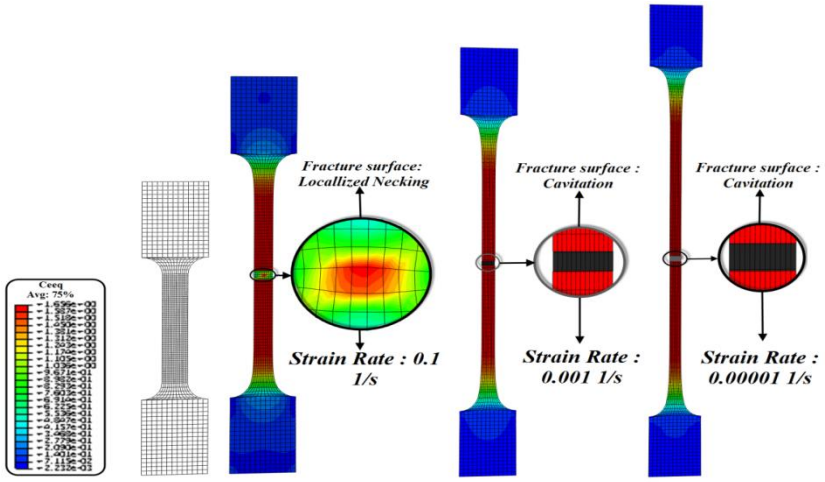

Fig.10. Deformed simple tensile test specimens at 450 ^{o}C at 10^{-1}, 10^{-3} and 10^{-5} s^{-1}.

Fig. 10 displays the fracture surfaces and the contours of equivalent creep strain of the samples deformed at these strain rates. It is observed that at high strain rate (10^{-1} s^{-1}), localized necking lead the sample to fracture. However, by decreasing the strain rate (at 10^{-3} and 10^{-5} s^{-1}) cavitation phenomenon is the factor of fracture.

The stress–strain curves at various temperatures is illustrated in Fig. 11. It appears that at lower strain after high initial stress, flow stress begins to gradually fall with strain, and at higher strain the flow stress is reached to a steady state stress. This kind of strain softening is normally observed when the material

exhibits continuous recrystallization during hot deformation where the deformed grains are replaced by strain free grain.

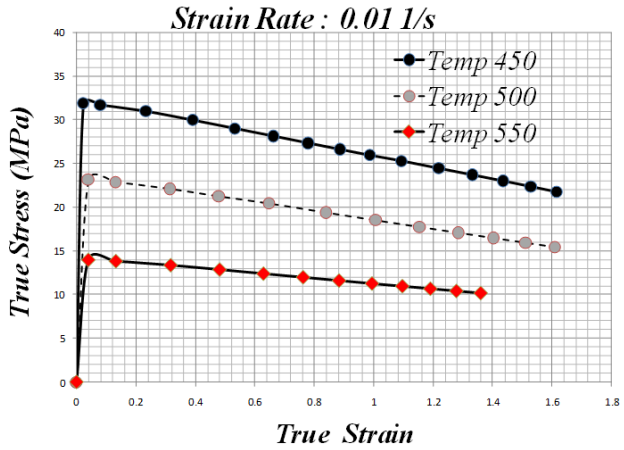

Fig.11. The stress- strain curves at various temperatures.

4. Conclusions

Finite element software ABAQUS v6.9 was used to predict the fracture of uniaxial superplastic tensile test of AA5083 alloy. It is shown that the proposed approach, which uses the instability criterion and cavitation, captures the characteristics of deformation and failure during superplastic forming. At low temperatures and high strain rates, the localized necking is the factor of fracture. However, at high temperatures and low strain rates, the cavitation is the main factor for sample fracture.

Acknowledgments: The authors would like to appreciate the office of the Vice President for Research of Babol Noshirvani University of Technology for financial supports.

5. References

[1] J. Pilling, N. Ridley, Superplasticity in Crystalline Solids, *The Institute of Metals*, 1989.

[2] C. H. Hamilton, A. K. Ghosh, *Superplastic sheet forming*, in: ASM Handbook, Vol. 14B, 2006.

[3] Y. H. Kim, S. S. Hong, J. S. Lee, R. H. Wagoner, Analysis of superplastic forming processes using a finite-element method, *Journal of Materials Processing Technology*, 62 (1996) 90–99.

[4] L. Carrino, G. Giuliano, C. Palmieri, Analysis of superplastic bulge forming by the finite element method, *Journal of Materials Processing Technology*, 16 (2001) 237–241.

[5] L. Carrino, G. Giuliano, W. Polini, A method to characterise superplastic materials in comparison with alternative methods, *Journal of Materials Processing Technology*, 138 (2003) 417–422.

[6] F. Shehata, M. J. Painter, R. Pearce, Warm forming of aluminum/magnesium alloy sheet, *Journal of Mechanical Working Technology*, 2 (1978) 279–290.

[7] T. Naka, G. Torikai, R. Hino, The effect of temperature and forming speed on the forming limit diagram for type 5083 aluminum-magnesium alloy sheet, *Journal of Materials Processing Technology*, 113 (2001) 648-653.

[8] S. J. Hosseinipour, An investigation into hot deformation of aluminum alloy 5083, *Materials and Design*, 30 (2009) 319–322.

[9] S. J. Hosseinipour, Strain rate sensitivity and cavitation in superplastic deformation of a commercial Al-5083 alloy, *Advanced Materials Research*, 83-86 (2010) 400-406.

[10] L. C. Chung, J. H. Cheng, Fracture criterion and forming pressure design for superplastic bulging, *Materials Science Engineering A*, 33 (2002) 146-151.

[11] R. Pearce, Superplasticity – an overview. Ashford Press, Curdridge, Southampton, Hampshire, 1989.

[12] Z. Marciniak, K. Kuczynski, Limit strain in the processes of stretch-forming sheet metals, *International Journal of Mechanical Science*, 9 (1967) 609.

[13] M. J. Stowell, Superplastic forming of structural alloys, In: Paton NE, Hamilton CH, editors. Warrendale: TMS-AIME, (1982) 321 –336.

[14] G. Giuliano, S. Franchitti, The determination of material parameters from superplastic free-bulging tests at constant pressure, *International Journal of Machine Tools and Manufacturing*, 48 (2008) 1519– 1522.

[15] D. Sorgente, L. D. Scintilla, Blow forming of AZ31 magnesium alloy at elevated temperatures, *International Journal of Materials Forming*, 3 (2010) 13–19.

[16] j. Liu, Z. Chen, H. Yan, Many-stage gas bulging forming of sheet magnesium alloy AZ31, *Metal Science and Heat Treatment*, 50 (2008) 110-114.

[17] M. Koç, E. Billur, An experimental study on the comparative assessment of hydraulic bulge test analysis methods, *Materials and Design*, 32 (2011) 272–281.

[18]. ABAQUS V.6.9 Documentation, Abaqus User Subroutines Reference Manual, section 1.1.17.